



Laboratoire Interdisciplinaire
Carnot de Bourgogne



Theoretical study of sodium D lines in a wide range of magnetic field with sub-Doppler resolution

Rodolphe MOMIER^{1,2}, Aram PAPOYAN², Claude LEROY¹

¹*Laboratoire Interdisciplinaire Carnot de Bourgogne, UMR CNRS 6303, Université Bourgogne Franche-Comté, 21000 Dijon, France*

²*Institute for Physical Research, National Academy of Sciences of Armenia, Ashtarak-2, 0203 Armenia*

momier.rodolphe@gmail.com

Contents

1. Spectroscopy with nanocells: an overview
2. Interaction of cw laser radiation with the vapor: linear interaction regime
3. Influence of the external magnetic field
4. Sodium D_2 line
5. Conclusion

1. Spectroscopy with nanocells: an overview

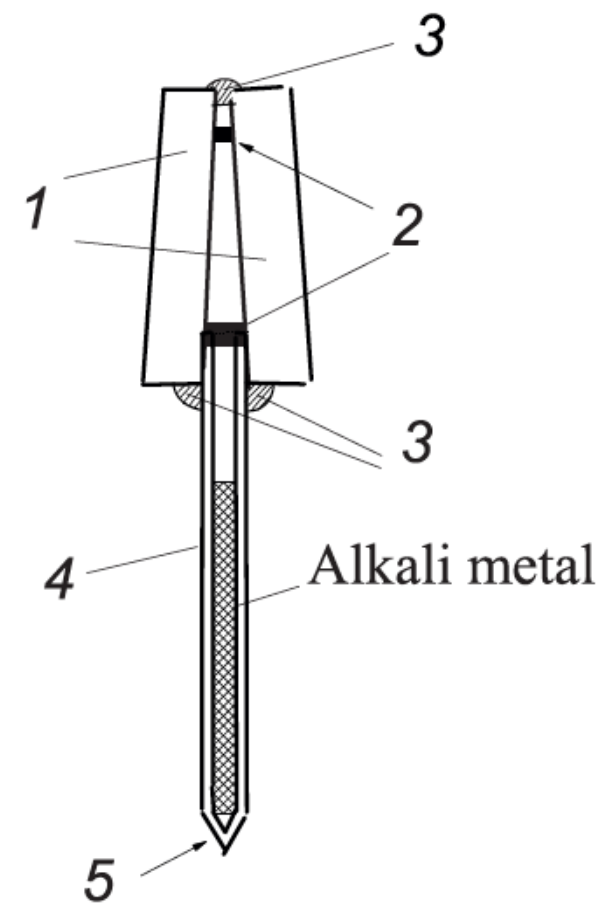


Fig.1: Typical scheme of a nanocell.
1: garnet or sapphire windows. 2: platinum or titanium strips. 3: high-temperature glue. 4: sapphire tube. 5: glass side-arm.



Fig.2: Picture of a nanocell. The interference profile arises from the reflection of the visible light on the internal surface of the cell (black arrow).

$$\tau = 1/\gamma = 16.249(19) \text{ ns for sodium } D_2 \text{ line}$$

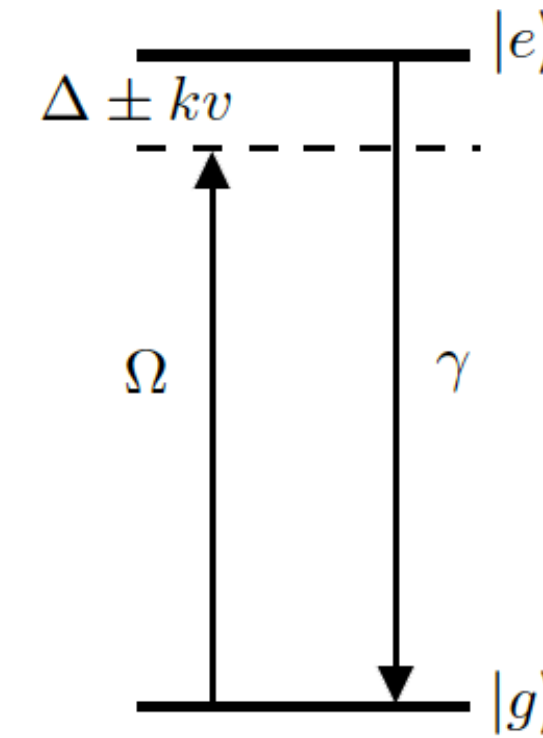
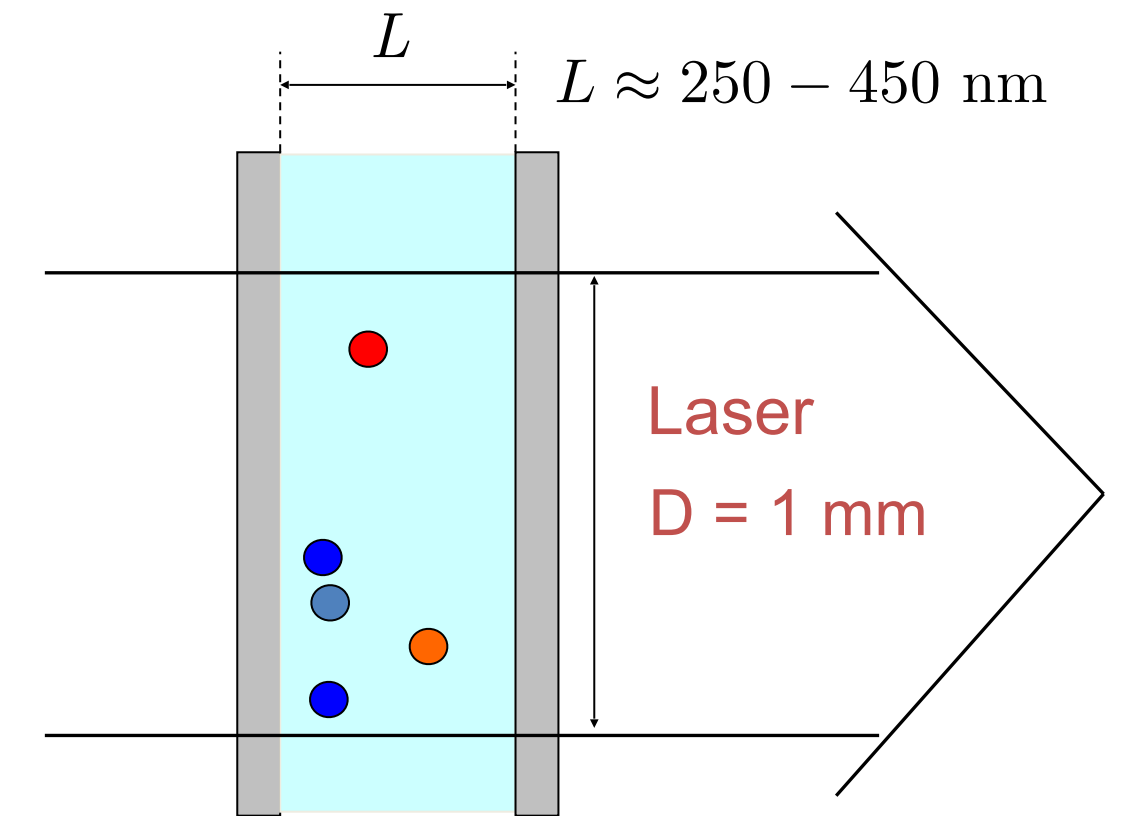


Fig. 3: Two-level system of lifetime τ .



$$t_D = D/v_p \approx 2 \mu\text{s}$$

$$t_L = L/v_p \approx 0.55 \text{ ns} \ll t_D$$

$$v_p \approx 545 \text{ m.s}^{-1} \text{ for sodium at } 140^\circ\text{C}$$

$$\begin{aligned} &\text{Doppler shift} \longrightarrow \text{Doppler broadening} \\ \omega &= \omega_L - \mathbf{k} \cdot \mathbf{v} = \omega_L \pm kv \\ &= \omega_L \pm \Delta_D \\ |\mathbf{k}| &\equiv k_z \end{aligned}$$

$$\gamma_D = \omega_0 \sqrt{\frac{8k_B T \ln 2}{m_a c^2}}$$

Only atoms such that
 $\mathbf{k} \cdot \mathbf{v} = 0$ (time of flight t_D)
 have time to interact.
 $\rightarrow \Delta_D = 0$ and $\gamma_D = 0$

D. Sarkisyan, D. Bloch, A. Papoyan and M. Ducloy, *Opt. Comm.* 200 201–208 (2001)

2. Interaction of cw laser radiation with the vapor

Linear interaction regime approximation

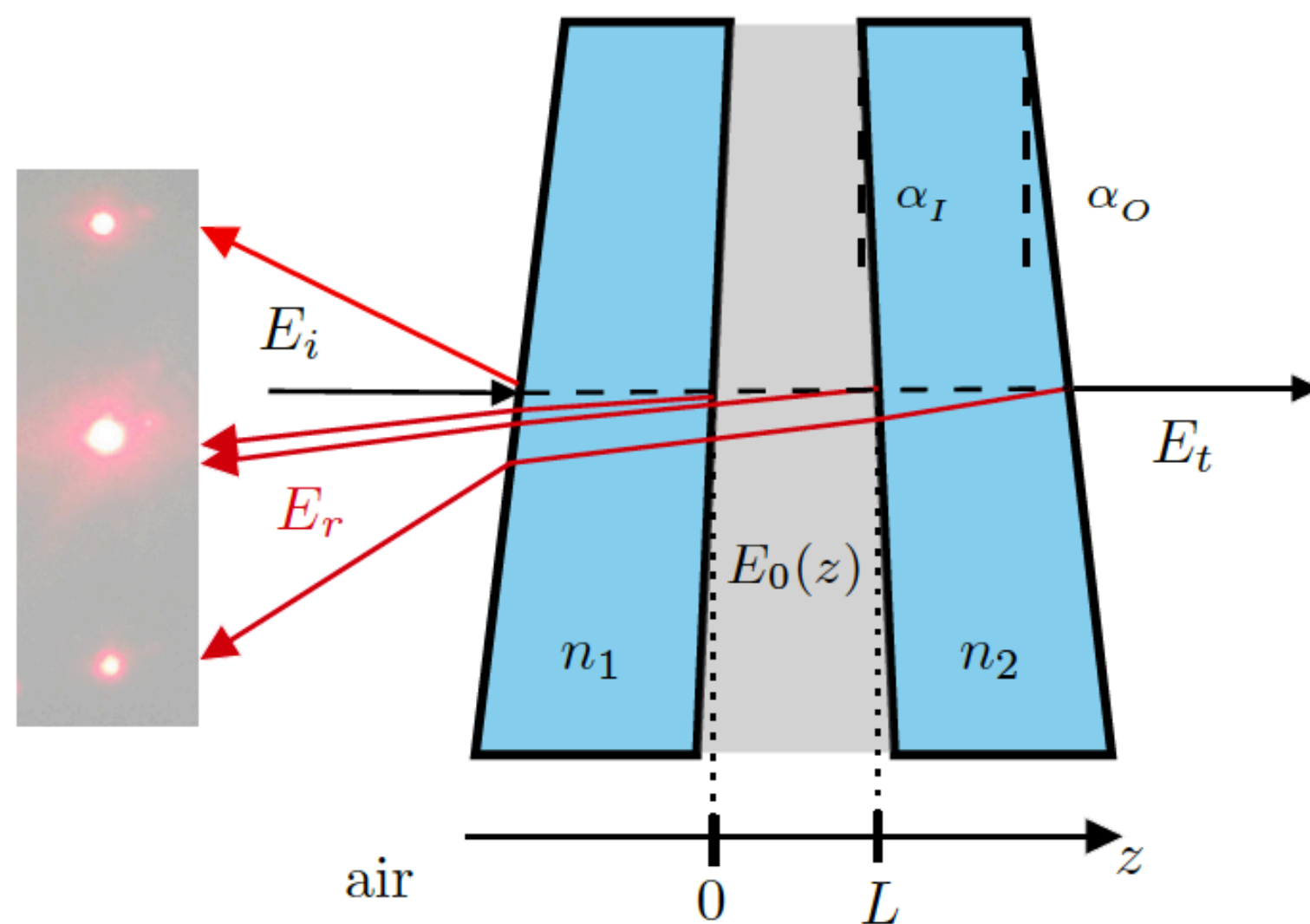


Fig. 4: Nanocell seen as a Fabry-Pérot interferometer

Atomic response

$$I_f = \frac{ik}{2\epsilon_0} \int_0^L P_0(z) dz \equiv I_T^{lin} - r_w I_{SR}^{lin}$$

$$I_b = \frac{ik}{2\epsilon_0} \int_0^L P_0(z) \exp(2ikz) dz \equiv I_{SR}^{lin} - r_w \exp(2ikL) I_T^{lin}$$

Transmitted and reflected signals

$$S_t \approx 2t_{wc} t_{cw}^2 E_i \text{Re}[I_f - r_w I_b] / |F|^2$$

$$S_r \approx 2t_{cw} E_i \text{Re} [r_w (1 - \exp(-2ikL)) \times (I_b - r_w I_f \exp(2ikL))] / |F|^2$$

G. Dutier, S. Saltiel, D. Bloch and M. Ducloy, JOSAB 20 5 (2003)

Interaction of cw laser radiation with the vapor

Linear interaction regime approximation

- Atom-surface collisions are neglected.
- Atoms leave the cell wall in the ground state.
- $D \gg L$
- Each Zeeman transition is seen as a two-level system, the contributions of each system are then added.

These approximations allow us to compute the transmitted and reflected signals without performing a complete numerical resolution of the density matrix equations.

3. Influence of the external magnetic field

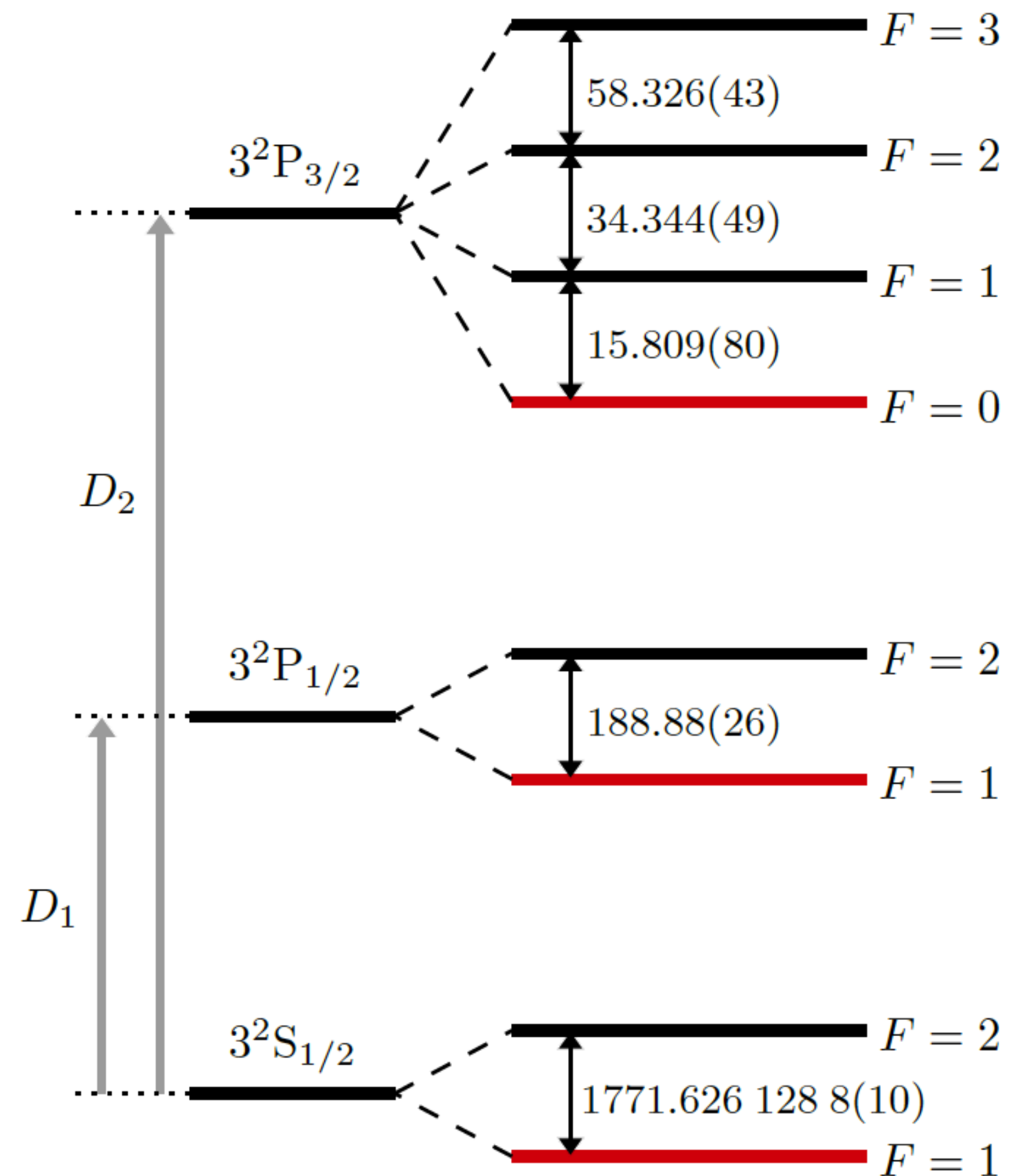


Fig. 5: Scheme of the energy levels of sodium D lines (splittings in MHz)

Inspired from D. Steck, Sodium D line data (2003)

Momier *et al.*

Zero-field Hamiltonian Magnetic contribution

$$\mathcal{H} = \mathcal{H}_0 + \mathcal{H}_m$$

$$\mathcal{H}_m = -\frac{\mu_B B_z}{\hbar} (g_L L_z + g_S S_z + g_I I_z)$$

L_z , S_z and I_z are the electronic orbital momentum, electronic spin momentum and nuclear spin momentum

Influence of the external magnetic field

Building the Hamiltonian matrices

Diagonal elements

$$\langle F, m_F | \mathcal{H} | F, m_F \rangle = E_0(F) - \mu_B g_F m_F B_z$$

Off-diagonal elements

$$\begin{aligned} \langle F - 1, m_F | \mathcal{H} | F, m_F \rangle &= \langle F, m_F | \mathcal{H} | F - 1, m_F \rangle \\ &= -\frac{\mu_B B}{2} (g_J - g_I) \sqrt{\frac{[(J - I + 1)^2 - F^2][F^2 - (J - I)^2]}{F}} \\ &\quad \times \sqrt{\frac{F^2 - m_F^2}{F(2F + 1)(2F - 1)}} \end{aligned}$$

*P. Tremblay, A. Michaud, M. Levesque, S. Thériault, M. Breton, J. Beaubien and N. Cyr, PRA **42** 5 2766-2773 (1990)*

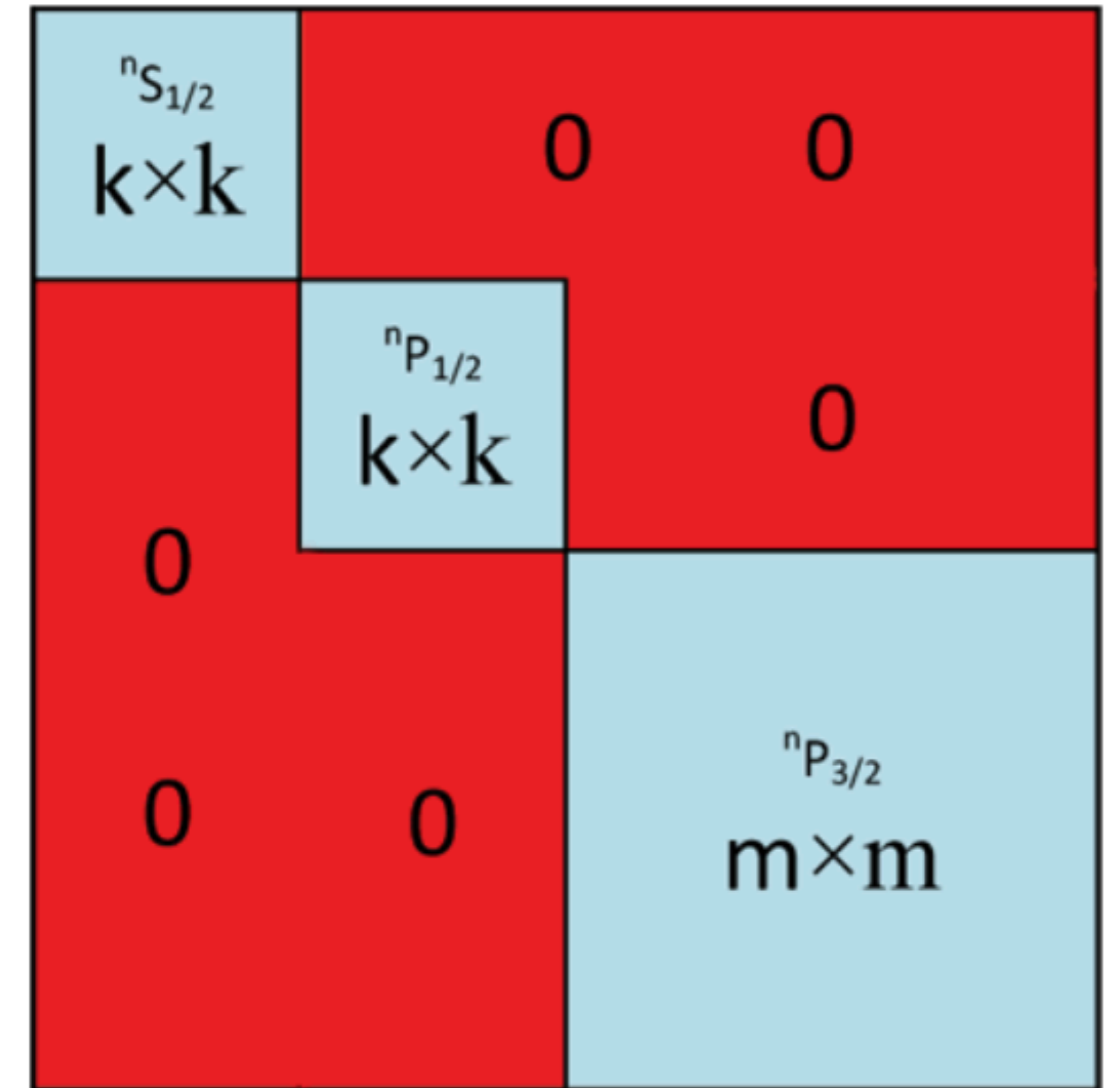


Fig. 6: Schematic representation of the block-diagonal Hamiltonian matrices

Influence of the external magnetic field

Transition intensities and frequency shifts

*P. Tremblay, A. Michaud, M. Levesque, S. Thériault, M. Breton, J. Beaubien and N. Cyr, PRA **42** 5 2766-2773 (1990)*

Eigenvectors of \mathcal{H} →

$$|\Psi(F, m_F)\rangle = \sum_{F'} \alpha_{F, F'}(B_z) |F', m_F\rangle$$

Transition intensity →

$$A_{eg} \propto a^2 [|\Psi(F_e, m_{F_e})\rangle; |\Psi(F_g, m_{F_g})\rangle; q]$$

Transfer coefficients modified by the presence of the magnetic field
 $q = 0, \pm 1$ for π, σ^\pm polarisation

$$A_{eg} \propto a^2 [|\Psi(F_e, m_{F_e})\rangle; |\Psi(F_g, m_{F_g})\rangle; q] = \left(\sum_{F'_e, F'_g} \alpha_{F_e, F'_e} a(F'_e, m_{F_e}; F'_g, m_{F_g}; q) \alpha_{F_g, F'_g} \right)^2$$

Unperturbed transfer coefficients →

$$a(F_e, m_{F_e}; F_g, m_{F_g}; q) = (-1)^{1+I+J_e+F_e+F_g-m_{F_e}}$$

$$\times \sqrt{2F_e+1} \sqrt{2F_g+1} \sqrt{2J_e+1} \begin{pmatrix} F_e & 1 & F_g \\ -m_{F_e} & q & m_{F_g} \end{pmatrix} \begin{Bmatrix} F_e & 1 & F_g \\ J_g & I & J_e \end{Bmatrix}.$$

Transition frequencies →

$$\omega_{eg} = \frac{\omega_e - \omega_g}{\hbar}$$

↓
3j and 6j Wigner symbols

4. Sodium D_2 line

Possible Zeeman transitions

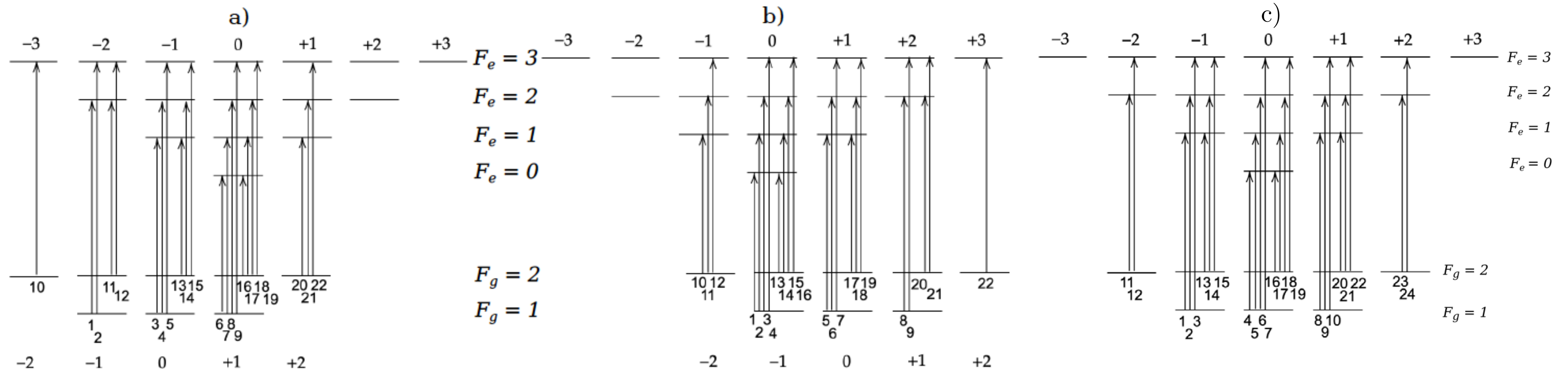


Fig. 7: All possible sodium D_2 line Zeeman transitions in the $|F, m_F\rangle$ basis.

a) σ^- -transitions. b) σ^+ -transitions. c) π -transitions

Sodium D_2 line

Transition intensities

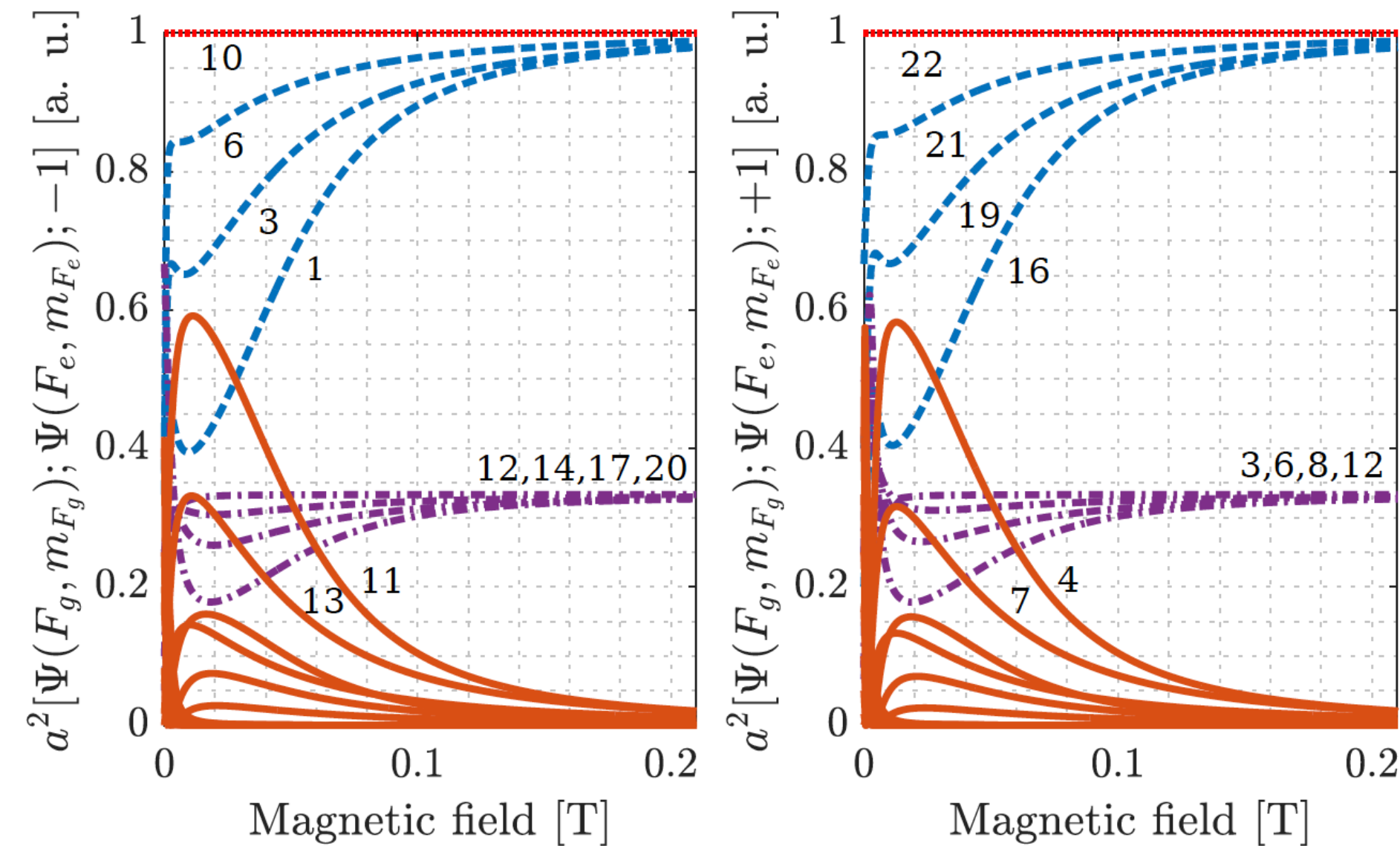


Fig. 8: Sodium D_2 line Zeeman σ -transitions intensities. **Left:** σ^- -transitions. **Right:** σ^+ -transitions. Two different groups of transitions remain past B_0 and are represented in blue dotted and purple dash-dotted lines. Red dotted lines: guiding transitions. Orange solid lines : vanishing transitions.

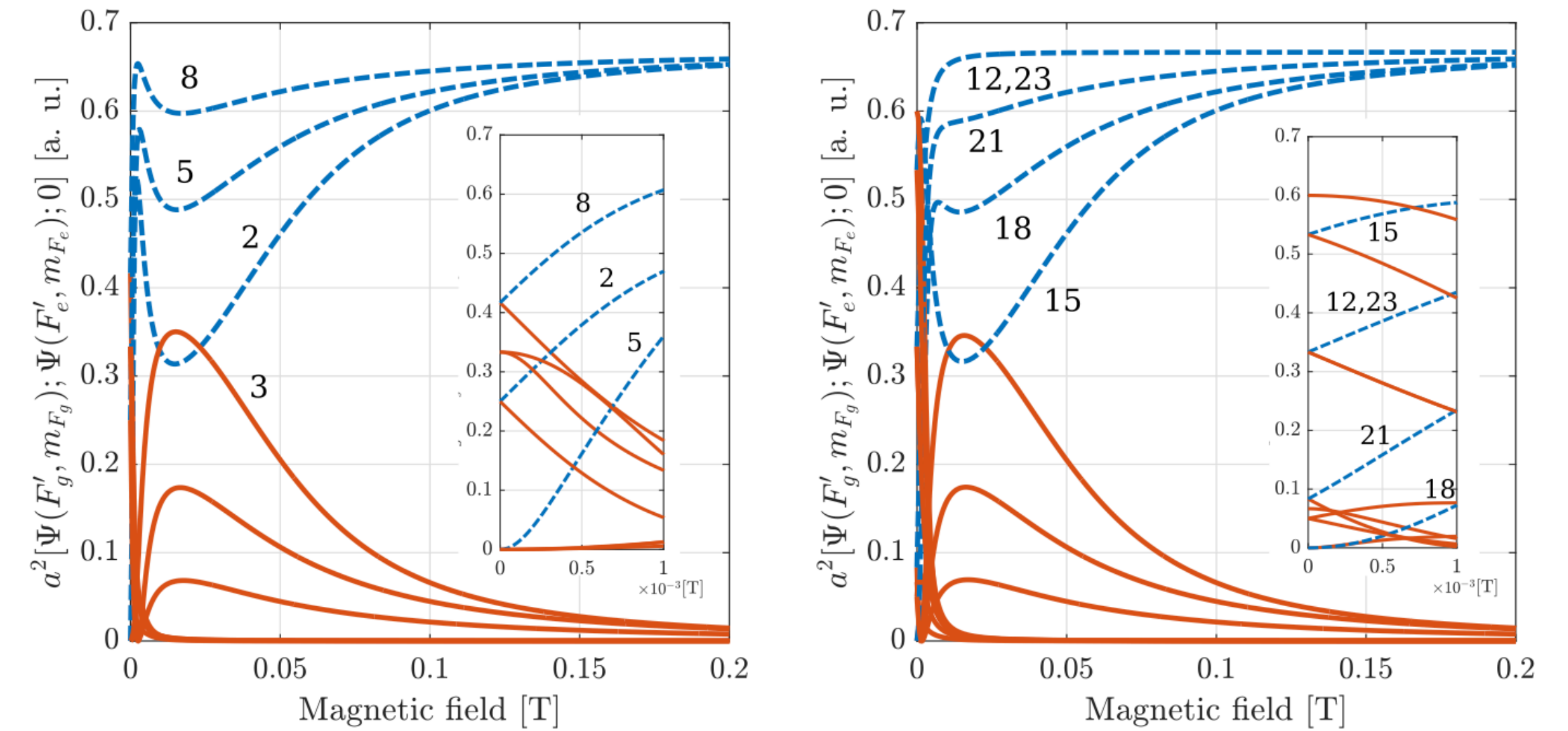


Fig. 9: Sodium D_2 line Zeeman π -transitions intensities. **Left:** Transitions from $F_g = 1$. **Right:** Transitions from $F_g = 2$. Same color code as before.

*R. Momier, A. Papoyan and C. Leroy, JQSRT **272** 107780 (2021)*

Sodium D_2 line

Circular polarization

Let's focus on σ -transitions now!

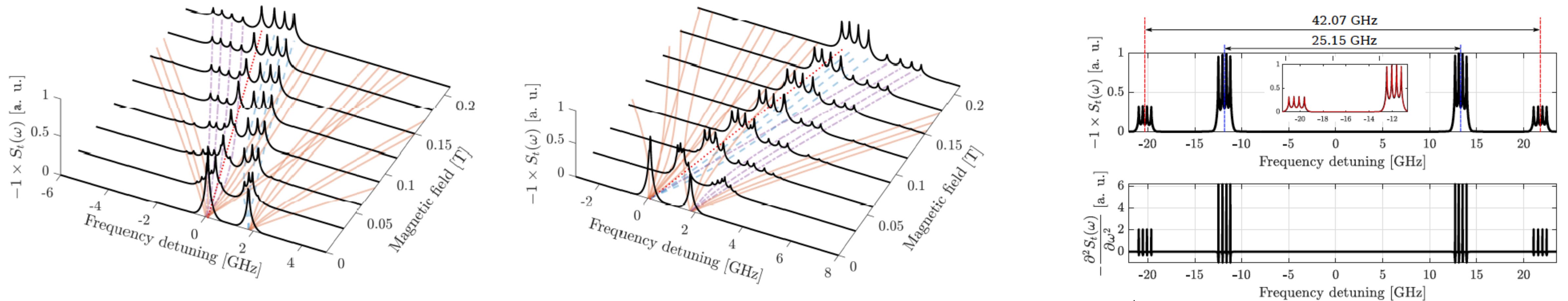


Fig. 10: Left: Absorption spectra of the D_2 line for σ^- -polarized incident laser radiation. **Center:** Absorption spectra of the D_2 line for σ^+ -polarized incident laser radiation. The magnetic field varies from 0 to 0.21 T with a step of 30 mT. The zero frequency corresponds to $F_g = 1 \rightarrow F_e = 0$. **Right:** Absorption spectrum in the hyperfine Paschen-Back regime ($B_z = 0.9$ T) and second derivative.

$$B_0(^{87}\text{Rb}) \approx 0.24 \text{ T} \quad B_0(^{133}\text{Cs}) \approx 0.16 \text{ T}$$

$$B_0(^{23}\text{Na}) \approx 0.063 \text{ T!}$$

Hyperfine Paschen-Back regime reached for $B_z > 10B_0$

R. Momier, A. Papoyan and C. Leroy, JQSRT **272** 107780 (2021)

Sodium D_2 line

Magnetically-induced circular dichroism

$$C_{MCD} = \frac{I^+ - I^-}{I^+ + I^-}$$

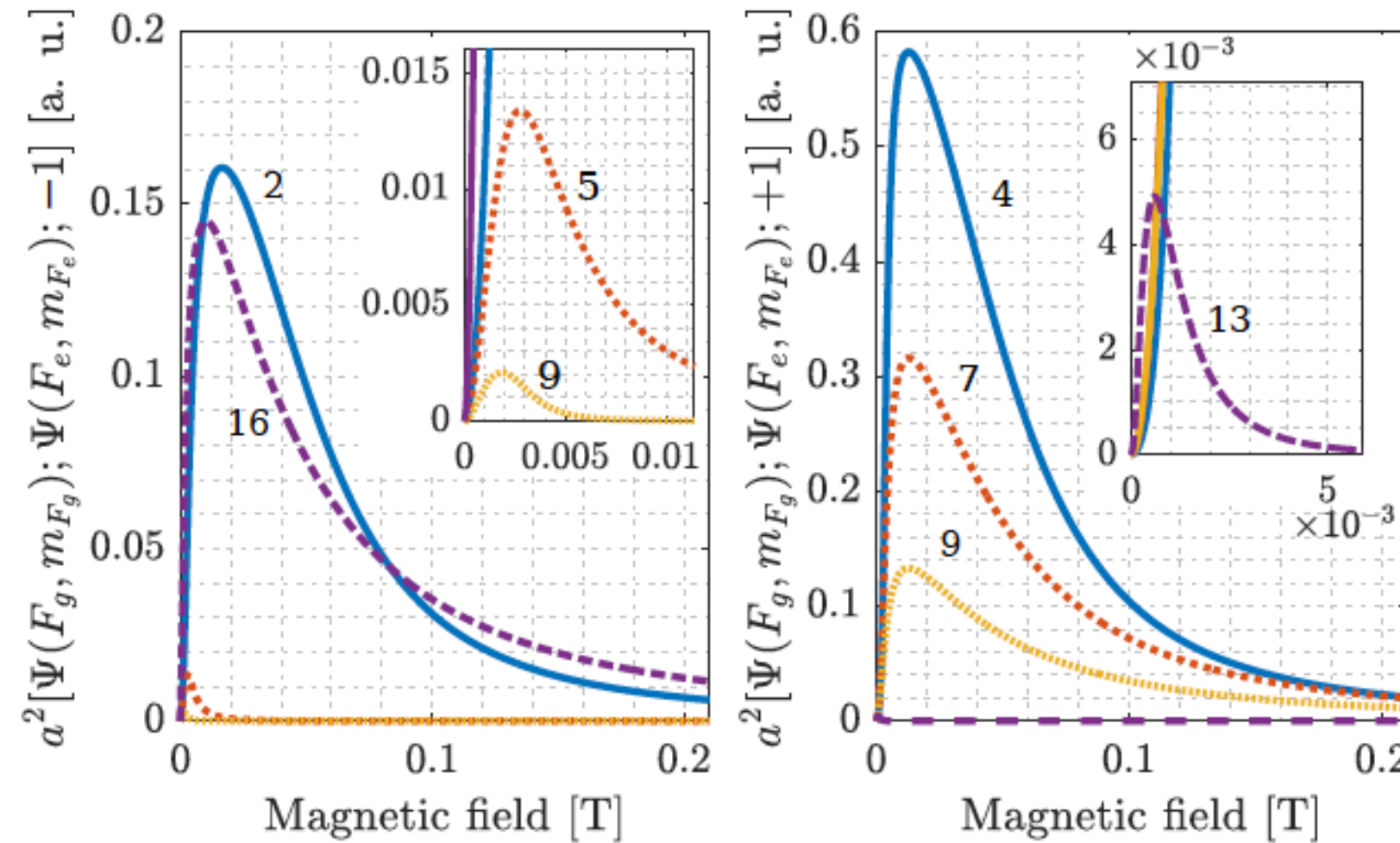
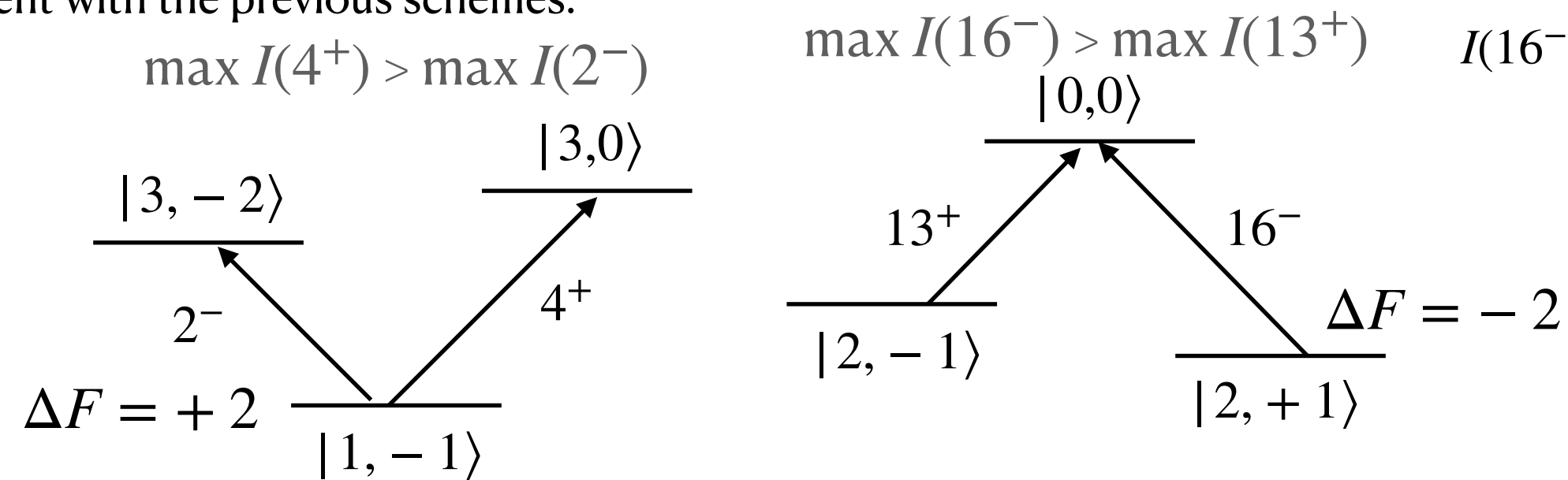


Fig. 11: Intensities of transitions obeying $\Delta F = \pm 2$. **Left:** σ^- -transitions. **Right:** σ^+ -transitions. The insets show the very-low-field behavior of transitions having a very small intensity. Labelling is consistent with the previous schemes.



R. Momier, A. Papoyan and C. Leroy, JQSRT **272** 107780 (2021)

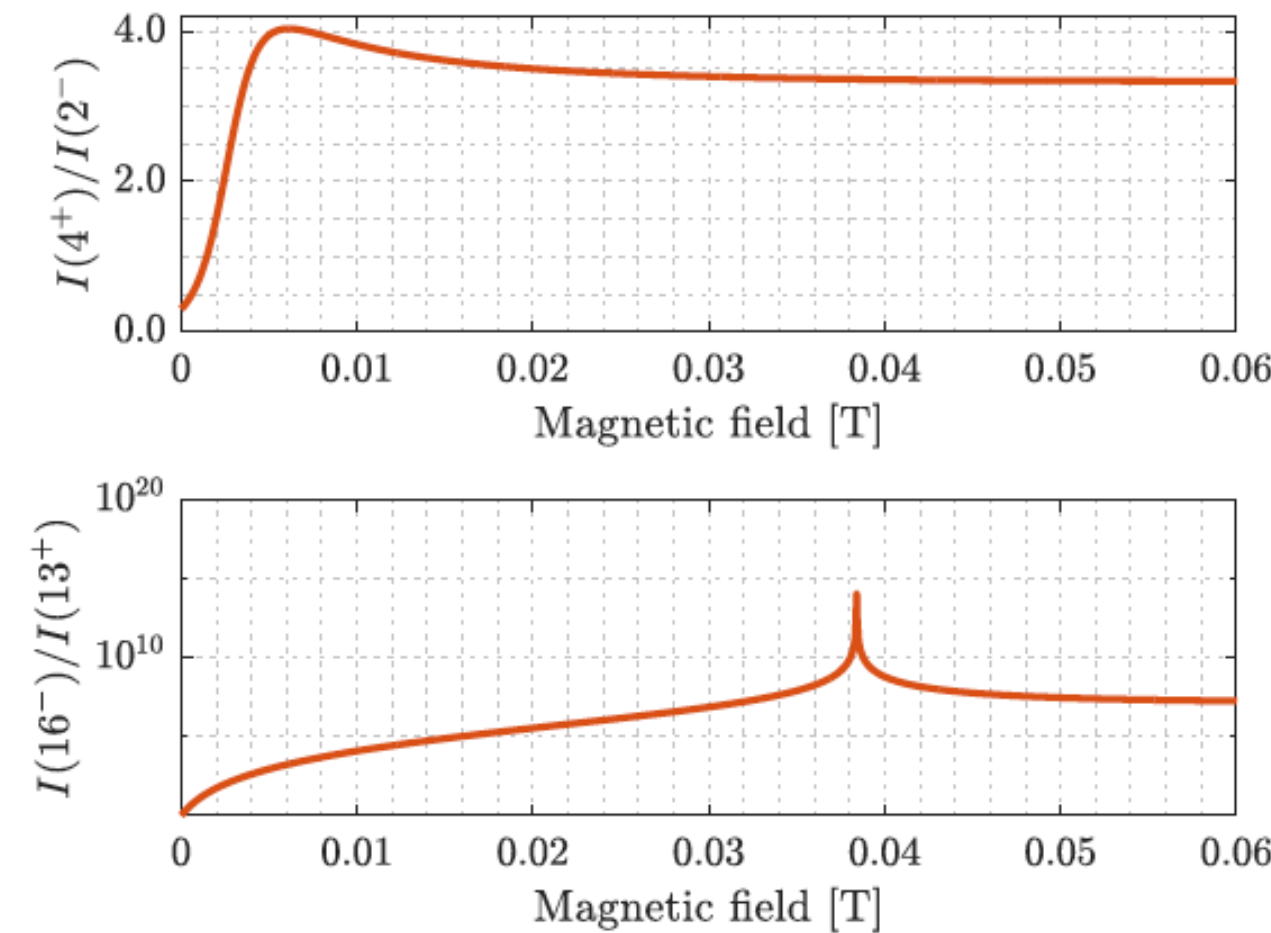


Fig. 12: Intensity ratio between the two strongest MI-transitions of their group. **Top panel:** MI-transitions obeying $\Delta F = +2$ (group $G2^+$, $I(4^+)/I(2^-)$). **Bottom panel:** MI-transitions obeying $\Delta F = -2$ (group $G2^-$, $I(16^-)/I(13^+)$).

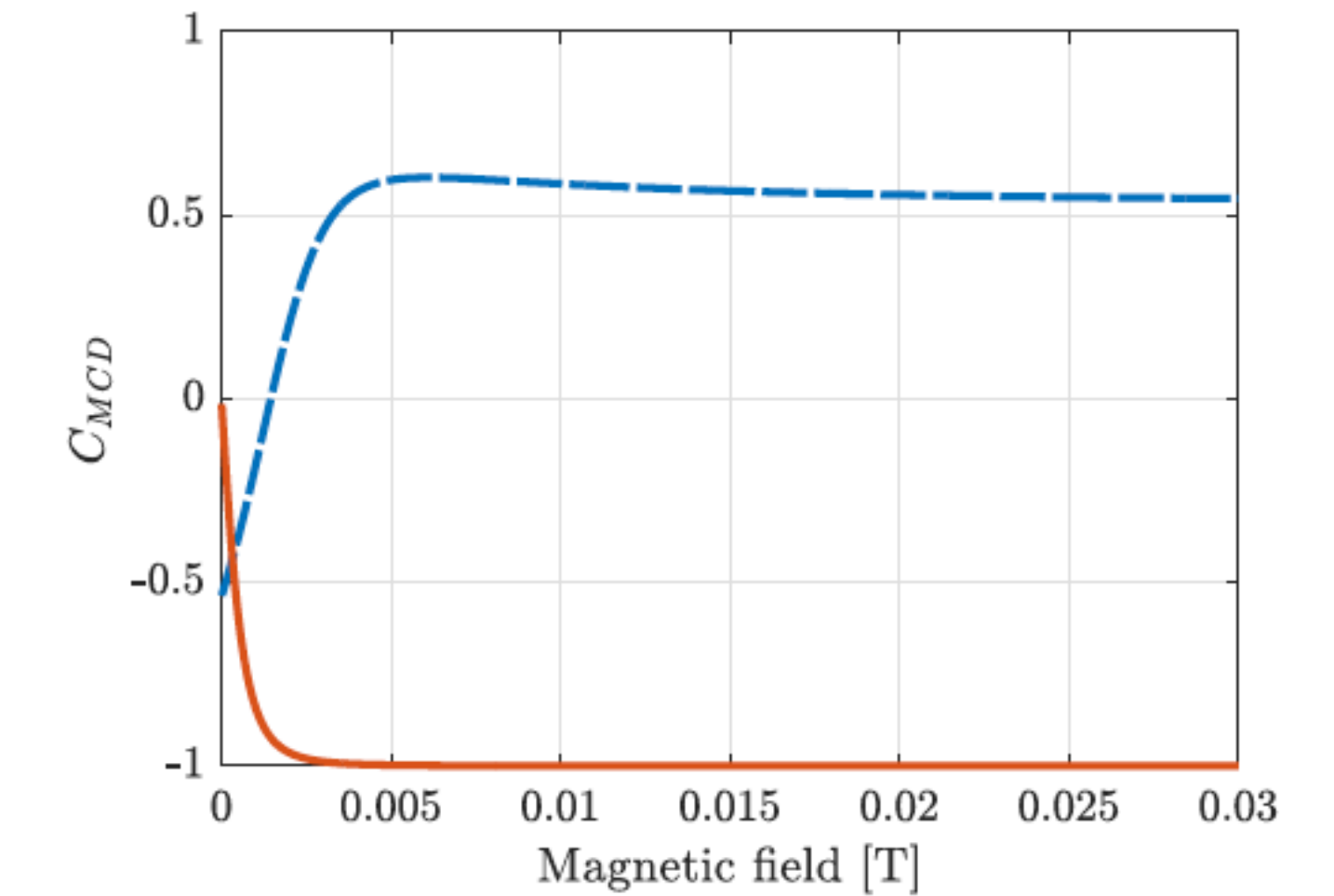


Fig. 13: Figure of merit coefficient C_{MCD} for each group of transitions. Blue (dashed) line: transitions 2^- and 4^+ . Orange solid line: transitions 16^- and 13^+ .

Type-1 MCD: MI transitions with $\Delta F = \pm 2$ are stronger when using σ^\pm radiation

Type-2 MCD: Among the strongest MI transitions (originating from different ground states) for σ^\pm polarization, the probability of MI transition with $\Delta F = +2$ is always greater than that of MI transition with $\Delta F = -2$. ($4^+ > 16^-$)

5. Conclusion and perspectives

- We described for the first time precise sub-Doppler spectral features of the D lines of sodium as well as the magneto-optical peculiarities that occur throughout the whole range of magnetic field.
- Sodium has a larger linewidth compared to other alkalis ($\Gamma_{nat}/2\pi \approx 10$ MHz, nearly twice bigger than for other alkali).
- Since sodium is lighter, its Doppler broadening γ_D is bigger (but “cancelled” when using nanocells):

$$\gamma_D = \omega_0 \sqrt{\frac{8k_B T \ln 2}{m_a c^2}}$$

- One expects total agreement between experiments and theory. Such aspects were thoroughly studied with K, Rb and Cs. (same quantum systems)
- Sodium D lines are much closer in frequency than K, Rb and Cs
 - We do not have a laser working in the wavelength range of Sodium yet, however we have the nanocell.
 - Planned high-temporal-resolution studies of resonant optical response in atomic vapor nanocells.
 - $B_0(\text{Na}) < B_0(\text{Rb}), B_0(\text{Cs})$: interesting candidate for studies occurring in the hyperfine Paschen-Back regime.

Thank you for your attention!